A hyperelastic visco-elasto-plastic damage model for rubber materials

Kai Oide*, Takaya Kobayashi*, and Junji Yoshida**

*Mechanical Design & Analysis Corporation
Tokyo, Japan

** University of Yamanashi
Yamanashi, Japan

Abstract: *In designing a kinetic mechanism for modern complex structural members that include a rubber device, it is of technical importance to improve the accuracy of predicting the inelastic cyclic behavior of rubber materials. A simple term like "dynamic spring constant" is no longer adequate to describe advanced industrial applications. This paper describes our experimental investigations and numerical simulations of the dynamic characteristics of rubber materials. The experimental dynamic responses, with strain amplitude, temperature dependence, or frequency dependence, were provided by simple shear test specimens as well as by automotive rubber bushings. The vibration test was performed by a shaking table with a sufficiently large load capacity for the frequency range of up to several tens of Hz. Reflecting the experimental results, a combined visco-elasto-plastic and hyperelastic damage model was implemented in a user subroutine of UMAT in Abaqus, which enabled representations of the visco-elastic, elasto-plastic, Mullins effect, and energy absorption performance of rubber materials. One of our aims is an application of the results of these investigations in the material-modeling working group of Japan Association for Nonlinear CAE (JANCAE). The working group sprang from the idea of providing a multidisciplinary forum for rubber researchers, design engineers, and software engineers through the medium of advanced finite element codes, including Abaqus. This paper also briefly describes JANCAE activities.*

Keywords: *Rubber Materials, Constitutive Model, Mullins' Effect, Strain-dependency, Hyperelastic, Visco-elasto-plastic, Damage, JANCAE*

1. Introduction

It is necessary to predict the mechanical behavior of structural members containing rubber materials with high accuracy. We developed the visco-elasto-plastic damage model for rubber materials considering the strain dependence and the frequency dependence for accurately reproducing the mechanical characteristics of rubber, such as stress propagation direction and energy absorbing capacity (Yoshida, 2015). This constitutive model combines a visco-elasto-plastic model and a hyperelastic damage model in parallel, and can reproduce the visco-elasticity, the elasto-plasticity, the Mullins effect, and the strain-dependency of the hysteretic loops for rubber material. In this study, which aims to apply this constitutive model to several specific problems, we created user subroutines for rubber material in the form of the user subroutine system, Unified Material Model Driver for rubber (UMMDr) (Terajima 2015).

The UMMDr is a system for simulating visco-elastic material models by using the user subroutines of commercial FEM codes. It has been created to work on the practical problems of nonlinear materials as a one of the activities of the working group of the Japan Association for Nonlinear CAE (President: Kenjiro Terada, Tohoku University), which is a non-profit organization (NPO JANCAE HP). In this activity, regardless of the respective positions and use codes, CAE engineers learn the basic theory of visco-elasticity, develop subroutines of material models, and verify them on their FEM software. The main participants are volunteers from the working group and engineers for some software vendors.

In this paper, first, we outline the framework of the UMMDr subroutine system for visco-elastic material models, then provide an overview of the visco-elasto-plastic damage model. In order to verify the behavior of the user subroutines, using Abaqus, we compare the experimental test results with the simulation test results, for the uni-axial tensile test, the equi-biaxial test, and the simple shear test for anti-vibration rubber. Finally, we apply it to industrial products in general.

2. The user subroutine system for visco-elastic material models

Figure 1 shows the framework of the user subroutine system UMMDr. The UMMDr, which is in the middle of Figure 1, is the material model driver that is a basic function of the subroutine for constitutive models. We can use this system by combining the isochoric components of the hyperelastic models, the damage models, and the visco-elastic models, and the volumetric components of the hyperelastic models, and then connecting the plugs-ins to each available code. Also, there is a program to drive UMMDr alone for verification, without linking to the commercial FEM codes. The items represented by grey shading in Figure 1 were shared among the volunteers, who developed subroutine programs and verified them. In the basic part of the UMMDr, the input is the deformation gradient tensor, which returns the stress tensor, tangent modulus, and state variables to the FEM code. The UMMDr, calculates the tangent modulus corresponding to the second Piola-Kirchhoff stress, which is based on the total Lagrangian formulation, but it is possible to calculate the tangent modulus corresponding to the updated Lagrangian formulation or the Jaumann stress rate, if necessary.

In the lower subroutines, variables are calculated depending on the material models, and the UMMDr receives them. For verification of each subroutine program, we compared the UMMDr responses with the theoretical responses of the biaxial tensile test, the simple shear test, and the pure expansion test. The volunteers preformed these tasks.

In the plug-in parts, the data for stress tensor, deformation gradient tensor, state variables, and the post data is exchanged between the FEM codes and the UMMDr. For verification of implemented subroutines into each FEM codes, we compared the responses of the UMMDr with the responses of one-element problems using the Ogden model for hyperelastic material, the Ogden and Roxburgh model (Ogden 1999) for damage material, and the Holzapfel model (Holzapfel 1996) for visco-elastic material. Also, some of the UMMDr responses were compared to the responses of FEM code. The engineers of some software vendors did these tasks.

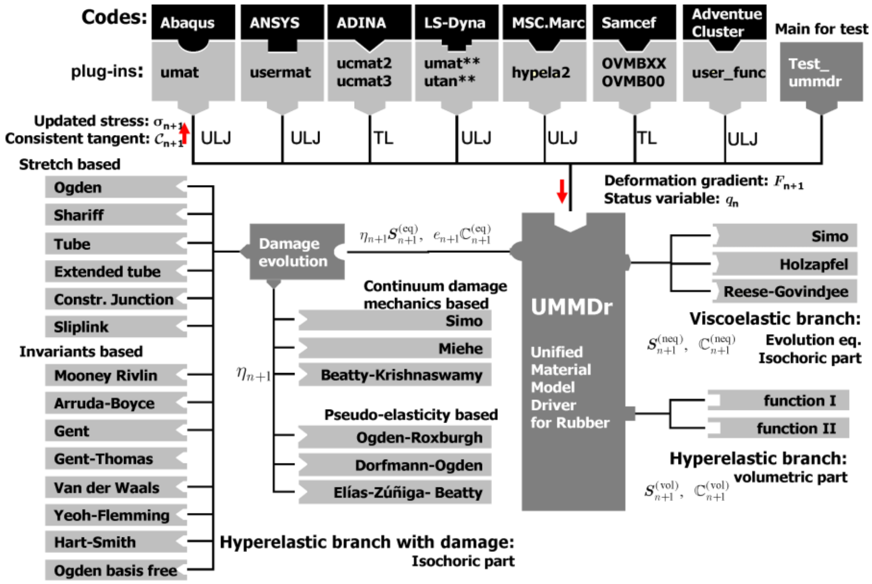

Figure 1. The framework of the user subroutine system UMMDr

3. Profile of the hyperelastic visco-elasto-plastic damage model

3.1 Free energy

This constitutive model consists of a hyperelastic damage element in parallel with visco-elasto-plastic elements (VEP elements) as shown Figure 2. The free energy for the entire model Φ is the sum of the free energy of the hyperelastic component Ψ_0 and the free energy of the visco-elasto-plastic component Ψ_k as

$$\Phi\left(\boldsymbol{E}, \boldsymbol{H}_k^{(e)}, d\right) = \Psi_0(\boldsymbol{E}, d) + \sum_{k=1}^{M} \Psi_k\left(\boldsymbol{H}(\boldsymbol{E}), \boldsymbol{H}_k^{(e)}\right),$$

where, d is the scalar variable which represents the damage, $\boldsymbol{E}$ is the Green-Lagrange strain tensor; $\boldsymbol{H}$ is the material logarithmic strain tensor, which is the function of $\boldsymbol{E}$; and $\boldsymbol{H}_k^{(e)}$ is the elastic material logarithmic strain tensor for the kth visco-elasto-plastic element.

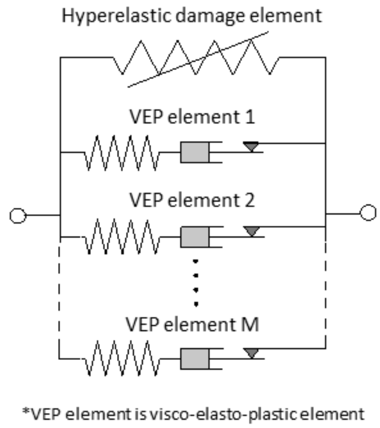

Figure 2. Elements of a hyperelastic visco-elasto-plastic damage model

3.2 Hyperelastic damage element

The free energy of the hyperelastic component Ψ_0 is divided to the isochoric deformation components $\overline{\Psi}_0$ and the volumetric deformation components U_0 as

$$\Psi_0 = \overline{\Psi}_0(\overline{\boldsymbol{C}}, d) + U_0(J).$$

Where $\overline{\boldsymbol{C}}$ is the isotropic component of the right Cauchy-Green deformation tensor $\boldsymbol{C}$; $\overline{\Psi}_0$ is given by d; and the free energy of isochoric deformation components without damage $\bar{\psi}_0$ as

$$\overline{\Psi}_0 = (1-d)\bar{\psi}_0(\overline{\boldsymbol{C}}).$$

In this paper, we use the Yamashita-Kawabata model (Yamashita 1992) for $\bar{\psi}_0$, with $\bar{I}_1, \bar{I}_2$ (the first and the second invariant of $\overline{\boldsymbol{C}}$) and the material coefficients c_1, c_2, c_3, n_0 as

$$\bar{\psi}_0 = c_1(\bar{I}_1 - 3) + c_2(\bar{I}_2 - 3) + \frac{c_3}{n_0 + 1}(\bar{I}_1 - 3)^{n_0+1}.$$

In this case, U_0 is given by κ_0 and volumetric rate J as

$$U_0 = \frac{\kappa_0}{2}(J-1)^2.$$

For the damage function, we use Ogden's pseudo-elastic model (Ogden 1999).
From the second law of thermodynamics, the second Piola-Kirchhoff stress tensor $\boldsymbol{S}_0$ resulting from the hyperelastic damage element is expressed as

$$\boldsymbol{S}_0 = \frac{\partial \Psi_0}{\partial \boldsymbol{E}} = (1-d) \cdot 2\frac{\partial \bar{\psi}_0}{\partial \boldsymbol{C}} + 2\frac{\partial U_0}{\partial \boldsymbol{C}}.$$

3.3 Visco-elasto-plastic element

For the free energy Ψ_k of the kth ($k = 1,2,\dots,M$) visco-elasto-plastic element, we use the product of the strain energy ψ_k and the hardening function Λ_k as

$$\Psi_k\left(\boldsymbol{H}, \boldsymbol{H}_k^{(e)}\right) = \Lambda_k(\boldsymbol{H}) \cdot \psi_k\left(\boldsymbol{H}_k^{(e)}\right).$$

Here, ψ_k is given by using the shear modulus $\mu_k^{(e)}$ and the isochoric deformation component $\boldsymbol{G}_k^{(e)}$ of $\boldsymbol{H}_k^{(e)}$ as

$$\psi_k = \bar{\psi}_k = \mu_k^{(e)} \left| \boldsymbol{G}_k^{(e)} \right|^2.$$

With reference to the Ogden's hyperelastic model, Λ_k is expressed using the principal values $\overline{\chi}_i (\mathrm{i} = 1{,}2{,}3)$ of $\overline{\boldsymbol{C}}$ and material coefficient m_k, h_k as

$$\Lambda_k = 1 + \frac{\overline{\chi}_1^{m_k/2} + \overline{\chi}_2^{m_k/2} + \overline{\chi}_3^{m_k/2} - 3}{m_k h_k}.$$

From the second law of thermodynamics, the stress tensor $\boldsymbol{T}_k$ resulting from the kth visco-elasto-plastic element is expressed as

$$\boldsymbol{T}_k = \frac{\partial \Psi_k}{\partial \boldsymbol{H}} + \frac{\partial \Psi_k}{\partial \boldsymbol{H}_k^{(e)}} = \boldsymbol{T}_k^{(1)} + \boldsymbol{T}_k^{(2)},$$

where $\boldsymbol{T}_k^{(1)} = \frac{\partial \Psi_k}{\partial \boldsymbol{H}_k^{(e)}},\ \boldsymbol{T}_k^{(2)} = \frac{\partial \Psi_k}{\partial \boldsymbol{H}}$. Here, $\boldsymbol{T}$ is the stress tensor, which is a work conjugate with the time derivative function of the material logarithmic strain tensor $\dot{\boldsymbol{H}}$, and is associated with a second Piola-Kirchhoff stress tensor by the fourth order tensor. The evolution of the non-elastic component is given by material parameters $\bar{\sigma}_k^{(0)}, \bar{\varepsilon}_k, N_k, \theta_k, \lambda_k$ as

$$\dot{\boldsymbol{H}} - \boldsymbol{H}_k^{(e)} = \left\{ (1 - \theta_k) \frac{\bar{\varepsilon}_k}{\lambda_k} + \theta_k (3K)^{\frac{1}{2}} \right\} \sqrt{\frac{2}{3}} (3\Omega_k)^{\frac{N_k}{2}} \boldsymbol{n}_k,$$

where $\widehat{\boldsymbol{T}}_k^{(1)} = \frac{\partial \bar{\psi}_k}{\partial \boldsymbol{H}_k^{(e)}},\ \boldsymbol{n}_k = \frac{\widehat{\boldsymbol{T}}_k^{(1)}}{\left| \widehat{\boldsymbol{T}}_k^{(1)} \right|},\ \Omega_k = \frac{\left| \widehat{\boldsymbol{T}}_k^{(1)} \right|^2}{2 \left(\bar{\sigma}_k^0 \right)^2},\ K = \frac{|\dot{\boldsymbol{G}}|^2}{2}$, and $\boldsymbol{G}$ is the isochoric deformation component of $\boldsymbol{H}$. The stress integration is carried out for the visco-plastic model, and eventually, resulting from the visco-elasto-plastic elements, the second Piola-Kirchhoff stress $\boldsymbol{S}_k$ is determined.

3.4 Stress in the hyperelastic visco-elasto-plastic damage model

The second Piola-Kirchhoff stress $\boldsymbol{S}$ is given as the sum of the stress of the hyperelastic damage element $\boldsymbol{S}_0$ and the stress of the visco-elasto-plastic element $\boldsymbol{S}_k$,

$$\boldsymbol{S} = \boldsymbol{S}_0 + \sum_{k=1}^{M} \boldsymbol{S}_k.$$

4. Finite element numerical simulation

4.1 Test for anti-vibration rubber material

After implementing the hyperelastic visco-elasto-plastic damage model in the UMMDr system, we verified the subroutine program by comparing the result to the test data for anti-vibration rubber material (Yoshida 2015). In this case, the number of the visco-elasto-plastic elements M was set to 3 and the material parameters in Table 1 were used. Using one element model, we did some numerical simulations for some material tests.

Table 1. Material parameters of the hyperelastic visco-elasto-plastic damage model for the anti-vibration rubber material test

Hyperelastic damage element	Parameter for $\bar{\psi}_0$: $c_1 = 0.326[\mathrm{N/mm^2}], c_2 = 0.0236[\mathrm{N/mm^2}], c_3 = 0.005[\mathrm{N/mm^2}], n_0 = 1.48$ Parameter of damage function: $r_0 = 0.649, m_0 = 1.89[\mathrm{N/mm^2}]$
VEP element 1	$\bar{\sigma}_1^{(0)} = 0.127[\mathrm{N/mm^2}], \bar{\varepsilon}_1 = 0.2, N_1 = 1.0, \theta_1 = 1.0, \lambda_1 = 1.0[\mathrm{sec}], m_1 = 1.32, h_1 = 0.382$
VEP element 2	$\bar{\sigma}_2^{(0)} = 1.29[\mathrm{N/mm^2}], \bar{\varepsilon}_2 = 1.0, N_2 = 1.07, \theta_2 = 0.0, \lambda_2 = 0.56[\mathrm{sec}], m_2 = 0.00119, h_2 = 45.1$
VEP element 3	$\bar{\sigma}_3^{(0)} = 0.528[\mathrm{N/mm^2}], \bar{\varepsilon}_3 = 1.0, N_3 = 2.51, \theta_3 = 0.0, \lambda_3 = 0.001[\mathrm{sec}], m_3 = 6.67, h_3 = 4.27$

Figure 3 shows the results of the uni-axial test, the equi-biaxial test, and the simple shear test. Red lines are experimental test results and blue lines are simulation results. From these figures, we can confirm that the user subroutine is implemented correctly.

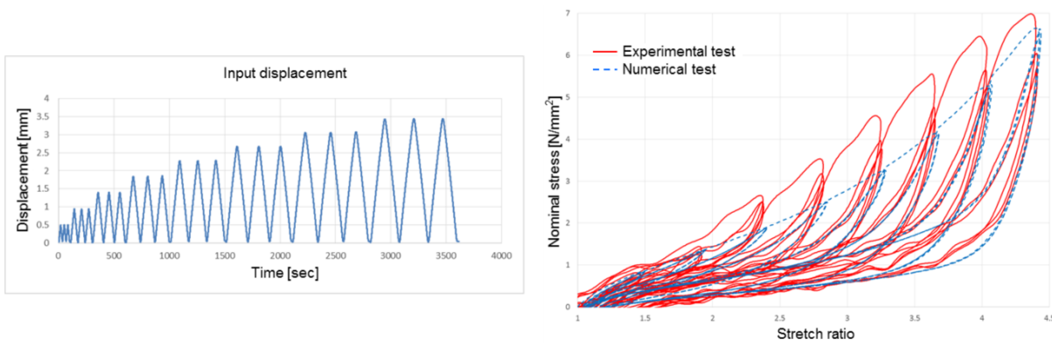

(a) uni-axial test

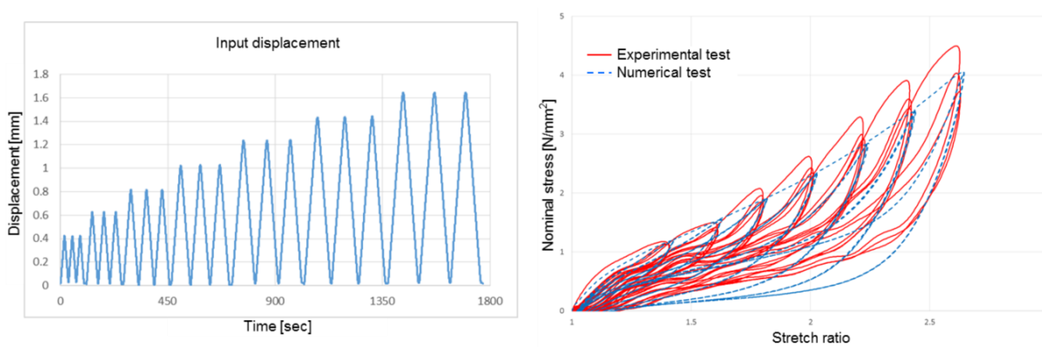

(b) equi-biaxial test

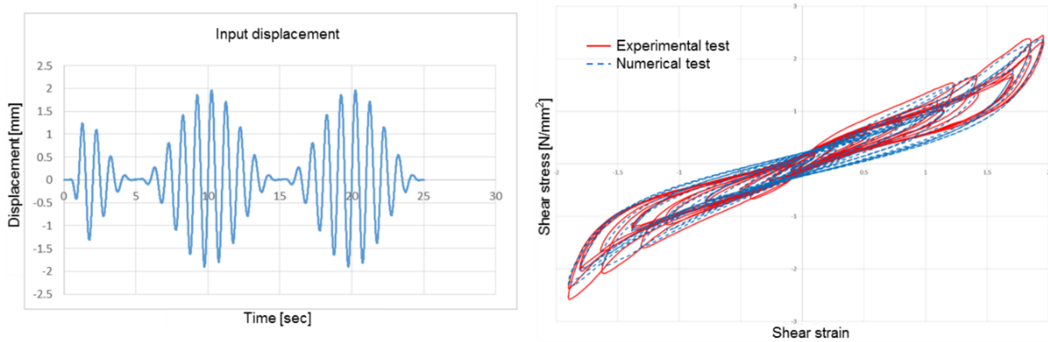

(c) simple shear test

Figure 3. Comparison of the results of the anti-vibration rubber material test and the numerical simulation

4.2 Rubber bushing load test

Consider the rubber bushing load tests shown Figure 4. In this case, it is hard to identify the rubber material parameters because some special testing machines are required for the material test. So, we used the rubber bushing load test results. Using the Isight optimization program, we identified the material parameters by minimizing the difference between the experimental loading results and the numerical loading results. Specifically, if $F_i(t_k)$ $(k = 1,2, \dots, M_i)$ is the ith $(i = 1,2, \dots, N)$ loading data, and $\hat{F}_i(t_k)$ is the corresponding FEM simulation data, the evaluation function E is

$$E = \frac{1}{N}\sum_{i=1}^{N}\left[\frac{1}{M_i F_{\max}^{(i)}}\sum_{k=1}^{M_i}\left|F_i(t_k) - \hat{F}_i(t_k)\right|\right].$$

$$F_{\max}^{(i)} = \max_{0\le k\le M_i}|F_i(t_k)|$$

The above equation was normalized using the maximum load for the experiment in order to deal with all test data equivalently, even though the test results are extremely different. In this model, there are 6 material parameters for the hyperelastic damage element and 7 for each of the visco-elasto-plastic elements. Because there are so many parameters, we used the parameters for the hyperelastic damage element without making any changes; we used the degenerated parameters for the visco-elastic-plastic element with considering some assumptions. Assuming that the first visco-elasto-plastic element represents elasto-plasticity, there are only 4 unknown material parameters ($\bar{\varepsilon}_1, \bar{\sigma}_1^{(0)}, m_1$, and h_1). Assuming that the kth visco-elasto-plastic element represents viscosity and rate dependency, there are 5 unknown material parameters ($\bar{\sigma}_k^{(0)}, N_k, \lambda_k, m_k$, and h_k). Based on the above assumptions, we identified the material parameters for the case of M = 3. Figures 5 and 6 show the results of the experimental and numerical simulations.

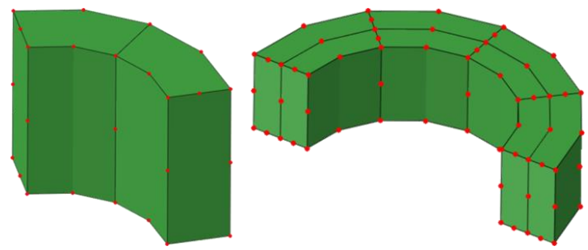

(a) Axial loading (b) Perpendicular loading

Figure 4. Simulation model of rubber bushings

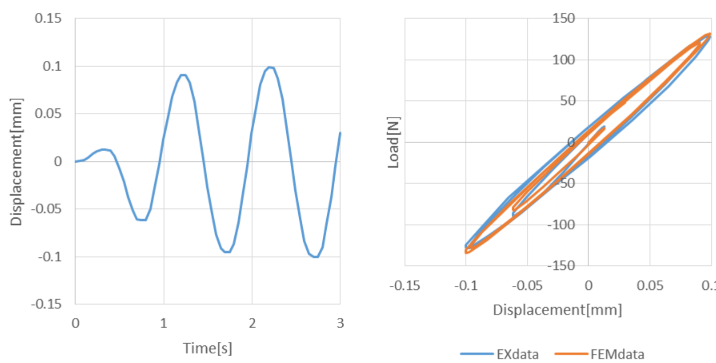

(a) Input displacement data (b) Load-Displacement curve

Figure 5. Results of experimental and numerical simulations for axial loading

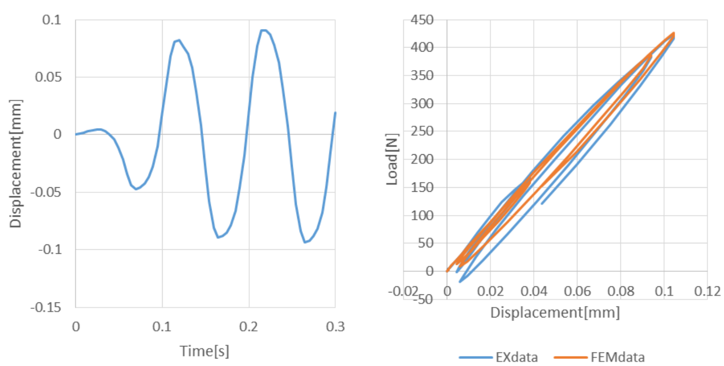

(a) Input displacement data (b) Load-Displacement curve

Figure 6. Results of experimental and numerical simulations for perpendicular direction axial loading

5. Conclusion

In this paper, we developed a user subroutine program for the hyperelastic visco-elasto-plastic damage model in the UMMDr system. Then, we verified it with experimental material test results and tested it using the rubber bushing load test. We used Abaqus 6.14 for the user subroutine and Isight2016 for identifying the material parameters.

6. References

1. Yoshida, J., and Sugiyama, T., "A Hyperelastic Visco-Elasto-Plastic Damage Model for Rubber-Like Solids including Strain Dependency of Hysteretic Loops," J. JSCE, A2, Vol. 71, No.1, 14-33, 2015.
2. Terajima, T., Takizawa, H., and Yoshida, J., "NPO Activity for Implementing Hyperelastic Damage–Viscoelastic Constitutive Models to Commercial FEM Codes," Proc. Conf. Comp. Eng. Science, Vol. 20, 2015.
3. non-profit organization Japan Association for Nonlinear CAE, HP: http://www.jancae.org/index.html
4. Ogden, R. W., and Roxburgh, D. G., "A Pseudo-Elastic Model for the Mullins Effect in Filled Rubber," The Royal Society of London, A-455, 2861-2877, 1999.
5. Holzapfel, G. A., "On large strain viscoelasticity: continuum formulation and finite element applications to elastomeric structures," Int. J. Num. Meth. Eng., Vol. 39, 3903-3926, 1996.
6. Yamashita, Y., and Kawabata, S., "Approximated form of the Strain Energy–Density Function of Carbon–Black Filled Rubbers for Industrial Applications," J. Society of Rubber Science and Technology, Japan, Vol. 65, No. 9, 517-528, 1992.